

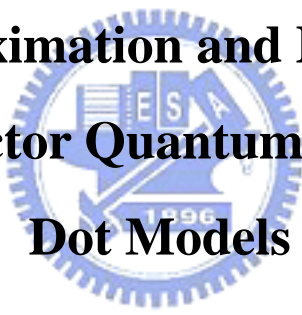
國立交通大學

應用數學系

碩士論文

半導體量子井、線、點模型的異質介面
近似方法與矩陣縮減方法

**Interface Approximation and Matrix Reduction
for Semiconductor Quantum Well, Wire, and
Dot Models**



研究生：高誠志

指導老師：劉晉良 教授

中華民國九十三年六月

半導體量子井、線、點模型的異質介面
近似方法與矩陣縮減方法

Interface Approximation and Matrix Reduction
for Semiconductor Quantum Well, Wire, and
Dot Models

研究生：高誠志

Student : Chen-Chih Kao

指導教授：劉晉良

Advisor : Jinn-Liang Liu



A Thesis

Submitted to Department of Applied Mathematics

College of Science

National Chiao Tung University

in Partial Fulfillment of the Requirements

for the Degree of

Master

in

Applied Mathematics

June 2004

Hsinchu, Taiwan, Republic of China

中華民國九十三年六月

半導體量子井、線、點模型的異質介面 近似方法與矩陣縮減方法

研究生：高誠志

指導老師：劉晉良博士

國立交通大學

應用數學系



在這一篇論文中，有二個部分。在第一個部分裡，我們討論了量子井 (quantum well)、量子線 (quantum wire)、量子點 (quantum dot) 的離散方法。我們使用不同的離散方法在模型中的異質介面條件 (interface condition) 上，並且去比較所得到的結果。因為異質介面條件是非常重要的，所以我們對它們使用不同的離散方法並且得到不同收斂行為結果的最小特徵值。在第二個部分裡，我們使用一些替代方法去縮減特徵值系統 $A \cdot x = \lambda \cdot x$ 中矩陣 A 的維度，而這樣所得到的最小特徵值會跟原矩陣 A 所求得的最小特徵值非常相近。這是因為其波函數 (wave function) 非常平順，所以當網格點非常細時在解整個系統就有一些不必要的計算。因此，我們使用了一些替代方法去縮減矩陣 A 的維度而我們仍然可以得到非常精確的最小特徵值。

Interface Approximation and Matrix Reduction for Semiconductor Quantum Well, Wire, and Dot Models

Student: Chen-Chih Kao

Advisor: Dr. Jinn-Liang Liu

*Department of Applied Mathematics
National Chiao Tung University*



There are two parts in the thesis. In the first part, we discuss the discretization in the quantum well, wire, and dot. For the interface condition, we use different discretizations to the model equation, and compare the results. Because the interface condition is very important, we use different discretizations to the interface condition and get different convergent results about the smallest eigenvalue. In the second part, we use some substitutions to reduce the dimension on the matrix A in the eigenvalue system $A \cdot x = \lambda \cdot x$, and get the smallest eigenvalue which is very close to the one of the original matrix A . Since the wave function can be very smooth, there is no need in solving the whole system with very fine mesh. Therefore, we use some substitutions to reduce the dimension of the matrix A and we can still get very accurate eigenvalue.

誌謝

首先我最要感謝我的指導教授 劉晉良 博士。劉教授他總是不厭其煩地引導我，教導我正確的研究方法與精神，讓我在求學過程中學習到許多寶貴的東西。真的非常感謝劉教授他的指導。同時我也要在此感謝本系博士班 陳人豪 學長在論文方面給了我許多的意見與幫助。

其次我要感謝我的朋友與研究所同學們，沒有他們的鼓勵與陪伴，我的研究所生活將會失色許多。

最後，我最特別要感謝我的父母與家人，由於他們的鼓勵與全力支持，我才能無後顧之憂地追求我的理想與完成我的學業，真的非常感激他們。



Contents

Abstract (in Chinese)	i
Abstract (in English)	ii
Acknowledgement	iii
Contents	iv
I Interface Approximations	1
1 Introduction	1
2 Linear Interface Approximation	2
2.1 Discretization	2
2.2 Matrix Formulation	3
3 Quadratic Interface Approximation	5
3.1 Discretization	5
3.2 Matrix Formulation	6
4 High Order Interface Approximation	7
4.1 Discretization	7
5 Quadratic Interface Approximation for 2D Model	9
5.1 Quadrangular Wire	9
5.1.1 Discretization	10
5.1.2 Matrix Formulation	10
5.2 Triangular Wire	12
5.2.1 Discretization	13
5.2.2 Matrix Formulation	13
6 Quadratic Interface Approximation for 3D Model	15
6.1 Quadrangular Dot	15
6.1.1 Discretization	16
6.1.2 Matrix Formulation	17
6.2 Truncated Octagonal-Based Pyramid Dot	19
6.2.1 Discretization	20
6.2.2 Matrix Formulation	21
7 Convergency of The Smallest Eigenvalue	24
7.1 1D Model	24
7.1.1 Convergency of Eigenvector	24
7.1.2 Convergency of Eigenvalue	25
7.2 2D Model	26

7.3	3D Model	27
8	Numerical Results	28
8.1	Linear Interface Approximation	28
8.2	Quadratic Interface Approximation	32
8.3	Quadratic Interface Approximation for 2D Model	35
8.3.1	Quadrangular Wire	35
8.3.2	Triangular Wire	37
8.3.3	The Direction of Interface Condition	38
8.4	Quadratic Interface Approximation for 3D Model	39
8.4.1	Quadrangular Dot	39
8.4.2	Truncated Octagonal-Based Pyramid Dot	41
II	Matrix Reduction	43
9	Introduction	43
10	Reduction of The Matrix	43
10.1	Positions of Deleted Point	43
10.2	Numbers of Deleted Point	43
11	Numerical Results	44
11.1	1D Model	44
11.2	2D Model	44
11.2.1	Quadrangular Wire	44
11.2.2	Triangular Wire	45
11.3	3D Model	46
11.3.1	Quadrangular Dot	46
11.3.2	Truncated Octagonal-Based Pyramid Dot	47
12	Conclusion	48
13	Reference	49

Part I

Interface Approximations

1 Introduction

In the world of quantum, the interesting problems are the problems in three-dimension (3D). But the complicated problems are always constructed from the simple problems. Thus, we start with simple finite well in one-dimension (1D), and we expect that the result of the finite well in 1D can bring some ideas and foundations for quantum dots in 3D and let us to understand semiconductor quantum dots more so that we can find more applications for our life, like quantum dot infrared photodetectors, lasers, etc. [7, 5].

For example, in the first part, we compare the discretizations for the equation of the interface condition. If we use linear interface approximation to the interface condition, we get the convergency of $O(h)$ for eigenvalue and eigenvector. If we use quadratic interface approximation, we get the convergency of $O(h^2)$ for eigenvalue and eigenvector. We find that the quadratic interface approximation is much better. Although we want to get better results, we use the high order interface approximation. However, if the order of interface approximation is higher than three, there are some problems with constructing the matrix. Therefore, all good results that we get are using quadratic interface approximation. With the experience of discretizations for interface condition, we also use quadratic interface approximation to 2D and 3D model. In order to solve the matrix of 2D and 3D model, we use Linear Jacobi-Davidson method [3, 8], since it can converge to the extreme eigenvalue quickly.

To deserve to be mentioned, there are some benefits with quadratic interface approximation. When we use quadratic interface approximation, we can construct the matrix which is symmetric. When we use the linear interface approximation, the place corresponding to the interface condition in the matrix is nonsymmetric and it is more expensive for solving the eigensystem. In addition to numerical verification, we also prove the convergence of the quadratic interface approximation for 1D, 2D, and 3D problem, and compare the different directions of interface condition for 2D model.

2 Linear Interface Approximation

We consider a single quantum well. According to *time-independent Schrödinger equation*, the model problem is:

$$-\frac{\hbar^2}{2m} \frac{d^2 u(x)}{dx^2} + V(x)u(x) = \lambda u(x); \quad x \in (a; b) \quad (2.1)$$

with the interface conditions:

$$\frac{1}{m_2} \frac{du}{dx} \Big|_{c^-} = \frac{1}{m_1} \frac{du}{dx} \Big|_{c^+}, \quad \frac{1}{m_1} \frac{du}{dx} \Big|_{d^-} = \frac{1}{m_2} \frac{du}{dx} \Big|_{d^+} \quad (2.2)$$

and the boundary conditions:

$$u(a) = u(b) = 0 \quad (2.3)$$

where $a < c < d < b$, $\hbar = \frac{h}{2\pi}$, h is Planck's constant, m_1 and m_2 are constant masses in $(c; d)$ and $(a; b) \setminus (c; d)$, respectively, $V(x)$ is the potential energy, as shown in Figure 2.1.

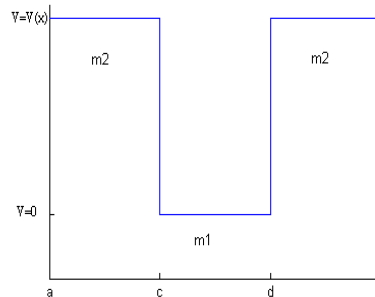


Figure 2.1. Structure schema of a single quantum well.

2.1 Discretization

There are two discretizations for the model equation. One is for grid points at the interface, and another is for grid points that satisfy (2.1). For (2.1), the discretization done by the central finite difference method is

$$\frac{d^2 u(x_i)}{dx^2} \approx \frac{u_{i-1} - 2u_i + u_{i+1}}{(M \Delta x)^2}$$

where $u_i = u(x_i)$, and $M \Delta x = x_i - x$. At the interface, we use the interface condition to substitute the model equation (2.1). The interface condition is as follows:

with

$$\alpha_k = \begin{cases} \frac{1}{m_2(Mx)^2} + V_{k,i} & 1 \leq k \leq \text{if1} - 2 \\ \frac{m_1 + 2m_2}{m_1 + m_2} \frac{1}{2m_2(Mx)^2} + V_{k,i} & k = \text{if1} - 1 \\ \frac{2m_1 + m_2}{m_1 + m_2} \frac{1}{2m_1(Mx)^2} & k = \text{if1} + 1 \\ \frac{1}{m_1(Mx)^2} & \text{if1} + 2 \leq k \leq \text{if2} - 2 \\ \frac{2m_1 + m_2}{m_1 + m_2} \frac{1}{2m_1(Mx)^2} & k = \text{if2} - 1 \\ \frac{m_1 + 2m_2}{m_1 + m_2} \frac{1}{2m_2(Mx)^2} + V_{k,i} & k = \text{if2} + 1 \\ \frac{1}{m_2(Mx)^2} + V_{k,i} & \text{if2} + 2 \leq k \leq n \end{cases}$$

$$\beta_k = \begin{cases} -\frac{1}{2m_2(Mx)^2} & 2 \leq k \leq \text{if1} - 1 \\ -\frac{1}{2m_1(Mx)^2} \frac{m_1}{m_1 + m_2} & k = \text{if1} + 1 \\ -\frac{1}{2m_1(Mx)^2} & \text{if1} + 2 \leq k \leq \text{if2} - 1 \\ -\frac{1}{2m_2(Mx)^2} \frac{m_2}{m_1 + m_2} & k = \text{if2} + 1 \\ -\frac{1}{2m_2(Mx)^2} & \text{if2} + 2 \leq k \leq n \end{cases}$$

$$\gamma_k = \begin{cases} -\frac{1}{2m_2(Mx)^2} & 1 \leq k \leq \text{if1} - 2 \\ -\frac{1}{2m_2(Mx)^2} \frac{m_2}{m_1 + m_2} & k = \text{if1} - 1 \\ -\frac{1}{2m_1(Mx)^2} & \text{if1} + 1 \leq k \leq \text{if2} - 2 \\ -\frac{1}{2m_2(Mx)^2} \frac{m_1}{m_1 + m_2} & k = \text{if2} - 1 \\ -\frac{1}{2m_2(Mx)^2} & \text{if2} + 1 \leq k \leq n - 1 \end{cases}$$

Note that A is nonsymmetric.

3 Quadratic Interface Approximation

In this case, we still use the model equation (2.1), but with different approximation for the interface condition.

3.1 Discretization

According to Taylor's expansion, we get the equation:

$$u_{i-1} \approx u_i + u_i^0(-Mx) + \frac{u_i^{00}}{2}(-Mx)^2$$

$$u_i^0 \approx \frac{u_i - u_{i-1}}{Mx} + \frac{u_i^{00}}{2}(Mx) \quad (3.1)$$

Similarly,

$$u_{i+1} \approx u_i + u_i^0(Mx) + \frac{u_i^{00}}{2}(Mx)^2$$

$$u_i^0 \approx \frac{u_{i+1} - u_i}{Mx} - \frac{u_i^{00}}{2}(Mx) \quad (3.2)$$

Because u satisfies (2.1) at $x_i \in c; d$, we get the equation

$$u_i^{00} = \left(\frac{2mV}{\sim 2} + \frac{-2m\lambda}{\sim 2} \right) u_i \quad (3.3)$$

From (3.1), (3.2), (3.3), the interface conditions (2.2) can be approximated by

$$\frac{1}{m_2} \left(\frac{u_i - u_{i-1}}{Mx} + \frac{Mx}{2} u_i^{00} \right) = \frac{1}{m_1} \left(\frac{u_{i+1} - u_i}{Mx} - \frac{Mx}{2} u_i^{00} \right)$$

$$\frac{u_i - u_{i-1}}{m_2 Mx} + \left(\frac{V_k Mx}{\sim 2} - \frac{\lambda Mx}{\sim 2} \right) u_i = \frac{u_{i+1} - u_i}{m_1 Mx} + \frac{\lambda Mx}{\sim 2} u_i$$

i.e.,

$$\frac{\sim 2}{2m_2(Mx)^2} u_{i-1} + \left(\frac{\sim 2}{2(Mx)^2} \frac{m_1 + m_2}{m_1 m_2} + \frac{V_k}{2} \right) u_i + \frac{\sim 2}{2m_1(Mx)^2} u_{i+1} = \lambda u_i \quad (3.4)$$

4 High Order Interface Approximation

If we further improve the order of the discretization at the interface and we would expect better results. But, unfortunately, we encounter some difficulties in doing this way.

4.1 Discretization

According to Taylor's expansion, we get the equation:

$$u_{i-1} \approx u_i + u_i^0(-Mx) + \frac{u_i^{00}}{2}(-Mx)^2 + \frac{u_i^{000}}{6}(-Mx)^3$$

$$u_i^0 \approx \frac{u_i - u_{i-1}}{Mx} + \frac{u_i^{00}}{2}(Mx) - \frac{(Mx)^2}{6}u_i^{000} \quad (4.1)$$

Similarly,

$$u_{i+1} \approx u_i + u_i^0(Mx) + \frac{u_i^{00}}{2}(Mx)^2 + \frac{u_i^{000}}{6}(Mx)^3$$

$$u_i^0 \approx \frac{u_{i+1} - u_i}{Mx} - \frac{u_i^{00}}{2}(Mx) - \frac{(Mx)^2}{6}u_i^{000} \quad (4.2)$$

From (3.3), we know that:

$$u_i^{00} = \left(\frac{2mV}{\hbar^2} + \frac{-2m\lambda}{\hbar^2} \right) u_i$$

and

$$u_i^{000} \Big|_{\text{well}^-} = (u_i^{00})^0 \quad (4.3)$$

$$= \left(\left(\frac{2mV}{\hbar^2} + \frac{-2m\lambda}{\hbar^2} \right) u_i \right)^0$$

$$= \left(\frac{2mV}{\hbar^2} + \frac{-2m\lambda}{\hbar^2} \right) \frac{u_i - u_{i-1}}{Mx}$$

$$u_i^{000} \Big|_{\text{well}^+} = (u_i^{00})^0 \quad (4.4)$$

$$= \left(\left(\frac{2mV}{\hbar^2} + \frac{-2m\lambda}{\hbar^2} \right) u_i \right)^0$$

$$= \left(\frac{2mV}{\hbar^2} + \frac{-2m\lambda}{\hbar^2} \right) \frac{u_{i+1} - u_i}{Mx}$$

From (3.3), (4.1), (4.2), (4.3), (4.4) the interface condition (2.2) can be approximated by

$$\begin{aligned} & \left(\frac{-1}{m_2(Mx)^2} + \frac{V_k}{3^{-2}} \right) u_{i-1} + \left(\frac{1}{(Mx)^2} \frac{m_1 + m_2}{m_1 m_2} + \frac{2V_k}{3^{-2}} \right) u_i + \left(\frac{-1}{m_1(Mx)^2} \right) u_{i+1} \\ & = \left(\frac{1}{3^{-2}} \right) \lambda u_{i-1} + \left(\frac{4}{3^{-2}} \right) \lambda u_i + \left(\frac{1}{3^{-2}} \right) \lambda u_{i+1} \end{aligned} \quad (4.5)$$

From (2.6), we know that there is a problem at the grid point in the interface when we are constructing the matrix.



5 Quadratic Interface Approximation for 2D Model

Because we use quadratic interface approximation to 1D problem and get good matrix formulation (A is symmetric) and numerical results, thus, we continue using the advantage of quadratic interface approximation to 2D problem.

5.1 Quadrangular Wire

We consider a quadrangular quantum wire which is embedded in the center of another quadrangular materials. According to *time-independent Schrödinger equation*, the 2D model problem is:

$$\frac{-\hbar^2}{2m} \Delta u(x; y) + V(x; y)u(x; y) = \lambda u(x; y) \quad (5.1)$$

with the interface conditions:

$$\begin{aligned} \frac{1}{m_2} \frac{\partial u}{\partial x} \Big|_{Q_{\text{left}}^-} &= \frac{1}{m_1} \frac{\partial u}{\partial x} \Big|_{Q_{\text{left}}^+}, & \frac{1}{m_1} \frac{\partial u}{\partial x} \Big|_{Q_{\text{right}}^-} &= \frac{1}{m_2} \frac{\partial u}{\partial x} \Big|_{Q_{\text{right}}^+} \\ \frac{1}{m_2} \frac{\partial u}{\partial y} \Big|_{Q_{\text{btm}}^-} &= \frac{1}{m_1} \frac{\partial u}{\partial y} \Big|_{Q_{\text{btm}}^+}, & \frac{1}{m_1} \frac{\partial u}{\partial y} \Big|_{Q_{\text{top}}^-} &= \frac{1}{m_2} \frac{\partial u}{\partial y} \Big|_{Q_{\text{top}}^+} \end{aligned} \quad (5.2)$$

and the boundary conditions:

$$u(X_{\text{left}}) = u(X_{\text{right}}) = 0$$

$$u(Y_{\text{btm}}) = u(Y_{\text{top}}) = 0 \quad (5.3)$$

as shown in Figure 5.1.

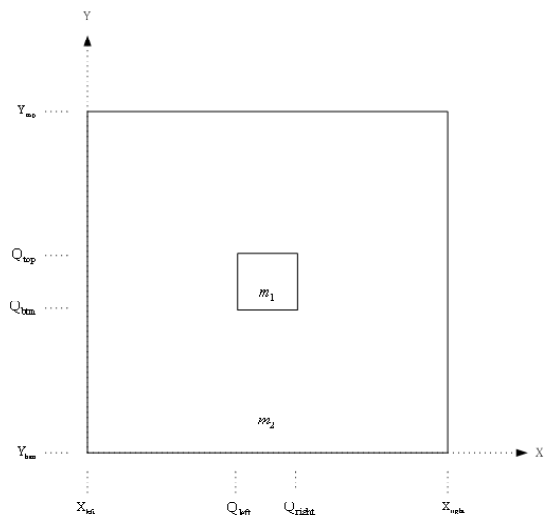


Figure 5.1. Structure schema of a quadrangular wire.

and the matrices $S_{i;k}$, $G_{i;k}$, $H_{i;k}$ are defined according to following three cases:

Case (i): If the matrices $S_{i;k}$, $G_{i;k}$, $H_{i;k}$ do not involve the interface and in mass m_2 ,

$$S_{i;k} = \begin{bmatrix} \alpha_1 & \gamma_1 & & & \\ \beta_2 & \alpha_2 & \gamma_2 & & \\ & \ddots & \ddots & \ddots & \\ & & \beta_{n-1} & \alpha_{n-1} & \gamma_{n-1} \\ & & & \beta_n & \alpha_n \end{bmatrix} \in \mathbb{R}^{n \times n} \quad (5.7)$$

and

$$G_{i;k} = -\frac{\sim^2}{2m_2(Mx)^2} I^{n \times n}, \quad H_{i;k} = -\frac{\sim^2}{2m_2(Mx)^2} I^{n \times n},$$

$$\text{with } \alpha_i = \frac{2 \sim^2}{m_2(Mx)^2} + V_i, \quad \beta_i = -\frac{\sim^2}{2m_2(Mx)^2}, \quad \gamma_i = -\frac{\sim^2}{2m_2(Mx)^2}.$$

Case (ii): If the matrices $S_{i;k}$, $G_{i;k}$, $H_{i;k}$ do not involve the interface and in mass m_1 , and the formulation of matrix $S_{i;k}$ is also (5.7), but with

$$G_{i;k} = -\frac{\sim^2}{2m_1(Mx)^2} I^{n \times n}, \quad H_{i;k} = -\frac{\sim^2}{2m_1(Mx)^2} I^{n \times n},$$

and

$$\alpha_i = \frac{2 \sim^2}{m_1(Mx)^2}, \quad \beta_i = -\frac{\sim^2}{2m_1(Mx)^2}, \quad \gamma_i = -\frac{\sim^2}{2m_1(Mx)^2}$$

Case (iii): If the matrices $S_{i;k}$, $G_{i;k}$, $H_{i;k}$ involve the interface, the matrices $S_{i;k}$, $G_{i;k}$, $H_{i;k}$ are chosen from the three cases described in Table 5.1.

Table 5.1
Possible choices of matrices $S_{i;k}$, $G_{i;k}$, $H_{i;k}$ involving interface.

Interface type	$S_{i;k}$		
	β_i	α_i	γ_i
Q_{left}	$-\frac{\sim^2}{2m_2(Mx)^2}$	$\frac{\sim^2}{2m_1(Mx)^2} + \frac{\sim^2}{2m_2(Mx)^2} + \frac{1}{2}V$	$-\frac{\sim^2}{2m_1(Mx)^2}$
Q_{right}	$-\frac{\sim^2}{2m_1(Mx)^2}$	$\frac{\sim^2}{2m_1(Mx)^2} + \frac{\sim^2}{2m_2(Mx)^2} + \frac{1}{2}V$	$-\frac{\sim^2}{2m_2(Mx)^2}$
Q_{btm}	0	$\frac{\sim^2}{2m_1(Mx)^2} + \frac{\sim^2}{2m_2(Mx)^2} + \frac{1}{2}V$	0
Q_{top}	0	$\frac{\sim^2}{2m_1(Mx)^2} + \frac{\sim^2}{2m_2(Mx)^2} + \frac{1}{2}V$	0

Interface type	$G_{i;k}$	$H_{i;k}$
Q_{left}	0	0
Q_{right}	0	0
Q_{btm}	$-\frac{\sim^2}{2m_2(Mx)^2} I^{n \times n}$	$-\frac{\sim^2}{2m_1(Mx)^2} I^{n \times n}$
Q_{top}	$-\frac{\sim^2}{2m_1(Mx)^2} I^{n \times n}$	$-\frac{\sim^2}{2m_2(Mx)^2} I^{n \times n}$

5.2 Triangular Wire

We consider a triangular quantum wire which is embedded in the center of another quadrangular materials. According to *time-independent Schrödinger equation*, the 2D model problem is:

$$\frac{-\hbar^2}{2m} \Delta u(x; y) + V(x; y)u(x; y) = \lambda u(x; y) \quad (5.8)$$

with the interface conditions:

$$\begin{aligned} \frac{1}{m_2} \frac{\partial u}{\partial x} \Big|_{T_{\text{left}}^-} &= \frac{1}{m_1} \frac{\partial u}{\partial x} \Big|_{T_{\text{left}}^+} \\ \frac{1}{m_1} \frac{\partial u}{\partial x} \Big|_{T_{\text{right}}^-} &= \frac{1}{m_2} \frac{\partial u}{\partial x} \Big|_{T_{\text{right}}^+} \end{aligned} \quad (5.9)$$

$$\frac{1}{m_2} \frac{\partial u}{\partial y} \Big|_{T_{\text{btm}}^-} = \frac{1}{m_1} \frac{\partial u}{\partial y} \Big|_{T_{\text{btm}}^+}$$

and the boundary conditions:

$$\begin{aligned} u(X_{\text{left}}) &= u(X_{\text{right}}) = 0 \\ u(Y_{\text{btm}}) &= u(Y_{\text{top}}) = 0 \end{aligned} \quad (5.10)$$

as shown in Figure 5.2.

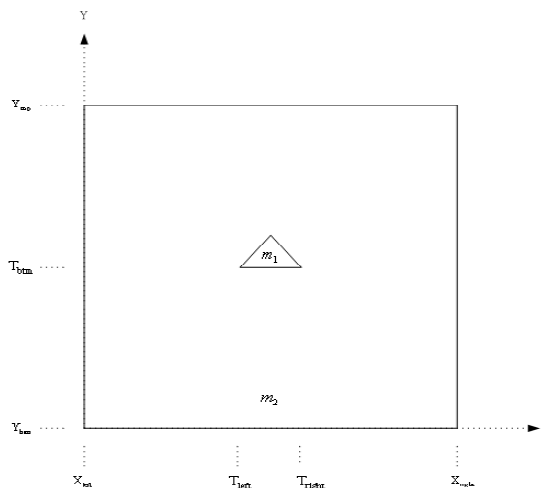


Figure 5.2. Structure schema of a triangular wire.

5.2.1 Discretization

With the same trick as for 1D model, the central finite difference approximation for (5.8) is thus

$$\frac{\Delta x^2}{2m} \left(\frac{u_{i-1,j} - 2u_{i,j} + u_{i+1,j}}{(\Delta x)^2} + \frac{u_{i,j-1} - 2u_{i,j} + u_{i,j+1}}{(\Delta y)^2} \right) + V_{i,j} u_{i,j} = \lambda u_{i,j} \quad (5.11)$$

where $u_{i,j} = u(x_i; y_j)$, $V_{i,j} = V(x_i; y_j)$ and $\Delta x = x_i - x_{i-1}$, $\Delta y = y_j - y_{j-1}$, $\Delta x = \Delta y$. And the interface conditions (5.9) with quadratic interface approximation can be approximated by

$$\frac{\Delta x^2}{2m_2} u_{i-1,j} + \left(\frac{\Delta x^2}{2m_1} + \frac{\Delta x^2}{2m_2} + \frac{V_k}{2} \right) u_{i,j} + \frac{\Delta x^2}{2m_1} u_{i+1,j} = \lambda u_{i,j}$$

$$\frac{\Delta x^2}{2m_1} u_{i-1,j} + \left(\frac{\Delta x^2}{2m_1} + \frac{\Delta x^2}{2m_2} + \frac{V_k}{2} \right) u_{i,j} + \frac{\Delta x^2}{2m_2} u_{i+1,j} = \lambda u_{i,j} \quad (5.12)$$

$$\frac{\Delta y^2}{2m_2} u_{i,j-1} + \left(\frac{\Delta y^2}{2m_1} + \frac{\Delta y^2}{2m_2} + \frac{V_k}{2} \right) u_{i,j} + \frac{\Delta y^2}{2m_1} u_{i,j+1} = \lambda u_{i,j}$$

5.2.2 Matrix Formulation

From (5.11), (5.12), we obtain the eigenvalue system (2.6) but with

$$A = \begin{pmatrix} S_{1;k} & H_{1;k} \\ G_{2;k} & S_{2;k} & H_{2;k} \\ \vdots & \vdots & \vdots \\ G_{n-1;k} & S_{n-1;k} & H_{n-1;k} \\ G_{n;k} & S_{n;k} \end{pmatrix} \in \mathbb{R}^{n^2 \times n^2}, U = \begin{pmatrix} F_{:,1} \\ F_{:,2} \\ \vdots \\ F_{:,n-1} \\ F_{:,n} \end{pmatrix} \in \mathbb{R}^{n^2 \times 1} \quad (5.13)$$

where

$$F_{:,k} = \begin{pmatrix} u_{1;k} \\ u_{2;k} \\ \vdots \\ u_{n-1;k} \\ u_{n;k} \end{pmatrix} \in \mathbb{R}^{n \times 1} \quad \text{for } k = 1; \dots; n$$

and the matrices $S_{i;k}$, $G_{i;k}$, $H_{i;k}$ are defined according to following three cases:

Case (i): If the matrices $S_{i;k}$, $G_{i;k}$, $H_{i;k}$ do not involve the interface and in mass m_2 ,

$$S_{i;k} = \begin{pmatrix} \alpha_1 & \gamma_1 & & & \\ \beta_2 & \alpha_2 & \gamma_2 & & \\ & \ddots & \ddots & \ddots & \\ & & \beta_{n-1} & \alpha_{n-1} & \gamma_{n-1} \\ & & & \beta_n & \alpha_n \end{pmatrix} \in \mathbb{R}^{n \times n} \quad (5.14)$$

and

$$G_{i;k} = -\frac{\sim^2}{2m_2(Mx)^2} I^{n \times n}; \quad H_{i;k} = -\frac{\sim^2}{2m_2(Mx)^2} I^{n \times n};$$

with $\alpha_i = \frac{2\sim^2}{m_2(Mx)^2} + V_i$, $\beta_i = -\frac{\sim^2}{2m_2(Mx)^2}$, $\gamma_i = -\frac{\sim^2}{2m_2(Mx)^2}$.

Case (ii): If the matrices $S_{i;k}$, $G_{i;k}$, $H_{i;k}$ do not involve the interface and in mass m_1 , and the formulation of matrix $S_{i;k}$ is also (5.14), but with

$$G_{i;k} = -\frac{\sim^2}{2m_1(Mx)^2} I^{n \times n}; \quad H_{i;k} = -\frac{\sim^2}{2m_1(Mx)^2} I^{n \times n};$$

and

$$\alpha_i = \frac{2\sim^2}{m_1(Mx)^2}, \quad \beta_i = -\frac{\sim^2}{2m_1(Mx)^2}, \quad \gamma_i = -\frac{\sim^2}{2m_1(Mx)^2}$$

Case (iii): If the matrices $S_{i;k}$, $G_{i;k}$, $H_{i;k}$ involve the interface, the matrices $S_{i;k}$, $G_{i;k}$, $H_{i;k}$, are chosen from the three cases described in Table 5.2.

Table 5.2
Possible choices of matrices $S_{i;k}$, $G_{i;k}$, $H_{i;k}$ involving interface.

Interface type	$S_{i;k}$		
	β_i	α_i	γ_i
T_{left}	$-\frac{\sim^2}{2m_2(Mx)^2}$	$\frac{\sim^2}{2m_1(Mx)^2} + \frac{\sim^2}{2m_2(Mx)^2} + \frac{1}{2}V$	$-\frac{\sim^2}{2m_1(Mx)^2}$
T_{right}	$-\frac{\sim^2}{2m_1(Mx)^2}$	$\frac{\sim^2}{2m_1(Mx)^2} + \frac{\sim^2}{2m_2(Mx)^2} + \frac{1}{2}V$	$-\frac{\sim^2}{2m_2(Mx)^2}$
T_{btm}	0	$\frac{\sim^2}{2m_1(Mx)^2} + \frac{\sim^2}{2m_2(Mx)^2} + \frac{1}{2}V$	0

Interface type	$G_{i;k}$	$H_{i;k}$
T_{left}	0	0
T_{right}	0	0
T_{btm}	$-\frac{\sim^2}{2m_2(Mx)^2} I^{n \times n}$	$-\frac{\sim^2}{2m_1(Mx)^2} I^{n \times n}$

6 Quadratic Interface Approximation for 3D Model

Because we want to understand semiconductor quantum dots more, we still continue using the advantage of quadratic interface approximation to 3D problem.

6.1 Quadrangular Dot

We consider a quadrangular quantum dot which is embedded in the center of another quadrangular materials. According to *time-independent Schrödinger equation*, the 3D model problem is:

$$\frac{-\hbar^2}{2m}\Delta u(x; y; z) + V(x; y; z)u(x; y; z) = \lambda u(x; y; z) \quad (6.1)$$

with the interface conditions:

$$\begin{aligned} \frac{1}{m_2} \frac{\partial u}{\partial x} \Big|_{Q_{\text{left}}^-} &= \frac{1}{m_1} \frac{\partial u}{\partial x} \Big|_{Q_{\text{left}}^+}, & \frac{1}{m_1} \frac{\partial u}{\partial x} \Big|_{Q_{\text{right}}^-} &= \frac{1}{m_2} \frac{\partial u}{\partial x} \Big|_{Q_{\text{right}}^+} \\ \frac{1}{m_2} \frac{\partial u}{\partial y} \Big|_{Q_{\text{fwd}}^-} &= \frac{1}{m_1} \frac{\partial u}{\partial y} \Big|_{Q_{\text{fwd}}^+}, & \frac{1}{m_1} \frac{\partial u}{\partial y} \Big|_{Q_{\text{bwd}}^-} &= \frac{1}{m_2} \frac{\partial u}{\partial y} \Big|_{Q_{\text{bwd}}^+} \\ \frac{1}{m_2} \frac{\partial u}{\partial z} \Big|_{Q_{\text{btm}}^-} &= \frac{1}{m_1} \frac{\partial u}{\partial z} \Big|_{Q_{\text{btm}}^+}, & \frac{1}{m_1} \frac{\partial u}{\partial z} \Big|_{Q_{\text{top}}^-} &= \frac{1}{m_1} \frac{\partial u}{\partial z} \Big|_{Q_{\text{top}}^+} \end{aligned} \quad (6.2)$$

and the boundary conditions:

$$\begin{aligned} u(X_{\text{left}}) &= u(X_{\text{right}}) = 0 \\ u(Y_{\text{fwd}}) &= u(Y_{\text{bwd}}) = 0 \\ u(Z_{\text{btm}}) &= u(Z_{\text{top}}) = 0 \end{aligned} \quad (6.3)$$

as shown in Figure 6.1.

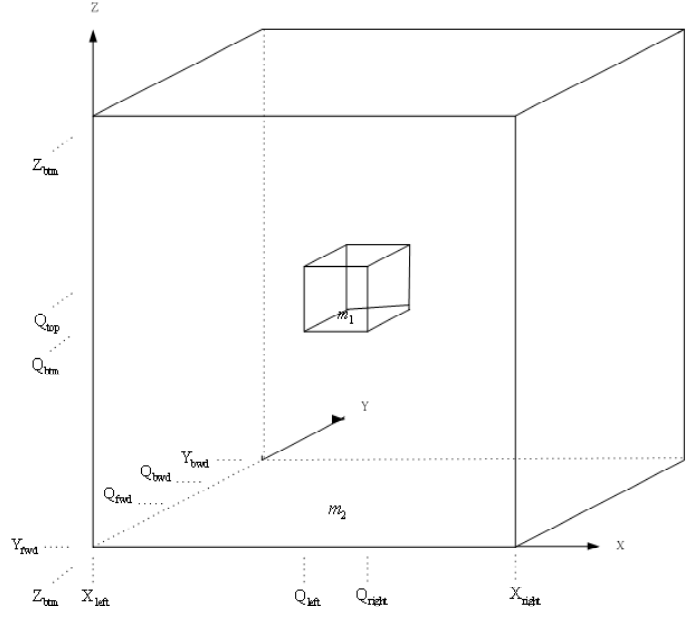


Figure 6.1. Structure schema of a quadrangular dot.

6.1.1 Discretization

With the same trick as for 1D model, the central finite difference approximation for (6.1) is thus

$$\frac{\Delta^2}{2m} \left(\frac{u_{i-1;j;k} - 2u_{i;j;k} + u_{i+1;j;k}}{(Mx)^2} + \frac{u_{i;j-1;k} - 2u_{i;j;k} + u_{i;j+1;k}}{(My)^2} + \frac{u_{i;j;k-1} - 2u_{i;j;k} + u_{i;j;k+1}}{(Mz)^2} \right) + V_{i;j;k}u_{i;j;k} = \lambda u_{i;j;k} \quad (6.4)$$

where $u_{i;j;k} = u(x_i; y_j; z_k)$, $V_{i;j;k} = V(x_i; y_j; z_k)$ and $Mx = x_i - x_{i-1}$, $My = y_j - y_{j-1}$, $Mz = z_k - z_{k-1}$, $Mx = My = Mz$. And the interface conditions (6.2) with quadratic interface approximation can be approximated by

$$\frac{\Delta^2}{2m_2(Mx)^2} u_{i-1;j;k} + \left(\frac{\Delta^2}{2m_1(Mx)^2} + \frac{\Delta^2}{2m_2(Mx)^2} + \frac{V_k}{2} \right) u_{i;j;k} + \frac{\Delta^2}{2m_1(Mx)^2} u_{i+1;j;k} = \lambda u_{i;j;k}$$

$$\frac{\Delta^2}{2m_1(My)^2} u_{i;j-1;k} + \left(\frac{\Delta^2}{2m_1(My)^2} + \frac{\Delta^2}{2m_2(My)^2} + \frac{V_k}{2} \right) u_{i;j;k} + \frac{\Delta^2}{2m_2(My)^2} u_{i;j+1;k} = \lambda u_{i;j;k}$$

$$\frac{\Delta^2}{2m_2(Mz)^2} u_{i;j;k-1} + \left(\frac{\Delta^2}{2m_1(Mz)^2} + \frac{\Delta^2}{2m_2(Mz)^2} + \frac{V_k}{2} \right) u_{i;j;k} + \frac{\Delta^2}{2m_1(Mz)^2} u_{i;j;k+1} = \lambda u_{i;j;k} \quad (6.5)$$

$$\frac{-\tilde{\omega}^2}{2m_1(My)^2} \mathbf{u}_{i,j-1;k} + \left(\frac{\tilde{\omega}^2}{2m_1(My)^2} + \frac{\tilde{\omega}^2}{2m_2(My)^2} + \frac{V_k}{2} \right) \mathbf{u}_{i,j;k} + \frac{-\tilde{\omega}^2}{2m_2(My)^2} \mathbf{u}_{i,j+1;k} = \lambda \mathbf{u}_{i,j;k}$$

$$\frac{-\tilde{\omega}^2}{2m_2(Mz)^2} \mathbf{u}_{i,j;k-1} + \left(\frac{\tilde{\omega}^2}{2m_1(Mz)^2} + \frac{\tilde{\omega}^2}{2m_2(Mz)^2} + \frac{V_k}{2} \right) \mathbf{u}_{i,j;k} + \frac{-\tilde{\omega}^2}{2m_1(Mz)^2} \mathbf{u}_{i,j;k+1} = \lambda \mathbf{u}_{i,j;k}$$

$$\frac{-\tilde{\omega}^2}{2m_1(Mz)^2} \mathbf{u}_{i,j;k-1} + \left(\frac{\tilde{\omega}^2}{2m_1(Mz)^2} + \frac{\tilde{\omega}^2}{2m_2(Mz)^2} + \frac{V_k}{2} \right) \mathbf{u}_{i,j;k} + \frac{-\tilde{\omega}^2}{2m_2(Mz)^2} \mathbf{u}_{i,j;k+1} = \lambda \mathbf{u}_{i,j;k}$$

6.1.2 Matrix Formulation

From (6.4), (6.5), we obtain the eigenvalue system (2.6) but with

$$A = \begin{pmatrix} T_1 & E_1 & & & \\ B_2 & T_2 & E_2 & & \\ & \ddots & \ddots & \ddots & \\ & & B_{n-1} & T_{n-1} & E_{n-1} \\ & & & B_n & T_n \end{pmatrix} \in \mathbb{R}^{n^3 \times n^3}, U = \begin{pmatrix} F_{\cdot\cdot\cdot 1} \\ F_{\cdot\cdot\cdot 2} \\ \vdots \\ F_{\cdot\cdot\cdot n-1} \\ F_{\cdot\cdot\cdot n} \end{pmatrix} \in \mathbb{R}^{n^3 \times 1} \quad (6.6)$$

where

$$B_k = \text{diag}[B_{1;k}, \dots, B_{n;k}] \in \mathbb{R}^{n^2 \times 1},$$

$$E_k = \text{diag}[E_{1;k}, \dots, E_{n;k}] \in \mathbb{R}^{n^2 \times 1},$$

$$T_k = \begin{pmatrix} S_{1;k} & H_{1;k} & & & \\ G_{2;k} & S_{2;k} & H_{2;k} & & \\ & \ddots & \ddots & \ddots & \\ & & G_{n-1;k} & S_{n-1;k} & H_{n-1;k} \\ & & & G_{n;k} & S_{n;k} \end{pmatrix} \in \mathbb{R}^{n^2 \times n^2},$$

$$F_{\cdot\cdot\cdot k} = \begin{pmatrix} u_{1;\cdot\cdot\cdot k} \\ u_{2;\cdot\cdot\cdot k} \\ \vdots \\ u_{n-1;\cdot\cdot\cdot k} \\ u_{n;\cdot\cdot\cdot k} \end{pmatrix} \text{ with } F_{i;\cdot\cdot\cdot k} = \begin{pmatrix} u_{i;\cdot\cdot\cdot k} \\ u_{i;\cdot\cdot\cdot k} \\ \vdots \\ u_{i;\cdot\cdot\cdot k} \\ u_{i;\cdot\cdot\cdot k} \end{pmatrix} \text{ for } k = 1, \dots, n,$$

Table 6.1
Possible choices of matrices $B_{i;k}$, $E_{i;k}$, $S_{i;k}$, $G_{i;k}$, $H_{i;k}$ involving interface.

Interface type	$S_{i;k}$		
	β_i	α_i	γ_i
Q_{left}	$-\frac{1}{2m_2(Mx)^2}$	$\frac{1}{2m_1(Mx)^2} + \frac{1}{2m_2(Mx)^2} + \frac{1}{2}V$	$-\frac{1}{2m_1(Mx)^2}$
Q_{right}	$-\frac{1}{2m_1(Mx)^2}$	$\frac{1}{2m_1(Mx)^2} + \frac{1}{2m_2(Mx)^2} + \frac{1}{2}V$	$-\frac{1}{2m_2(Mx)^2}$
Q_{fwd}	0	$\frac{1}{2m_1(Mx)^2} + \frac{1}{2m_2(Mx)^2} + \frac{1}{2}V$	0
Q_{bwd}	0	$\frac{1}{2m_1(Mx)^2} + \frac{1}{2m_2(Mx)^2} + \frac{1}{2}V$	0
Q_{btm}	0	$\frac{1}{2m_1(Mx)^2} + \frac{1}{2m_2(Mx)^2} + \frac{1}{2}V$	0
Q_{top}	0	$\frac{1}{2m_1(Mx)^2} + \frac{1}{2m_2(Mx)^2} + \frac{1}{2}V$	0

Interface type	$B_{i;k}$	$G_{i;k}$	$H_{i;k}$	$E_{i;k}$
Q_{left}	0	0	0	0
Q_{right}	0	0	0	0
Q_{fwd}	0	$-\frac{1}{2m_2(Mx)^2} I^{n \times n}$	$-\frac{1}{2m_1(Mx)^2} I^{n \times n}$	0
Q_{bwd}	0	$-\frac{1}{2m_1(Mx)^2} I^{n \times n}$	$-\frac{1}{2m_2(Mx)^2} I^{n \times n}$	0
Q_{btm}	$-\frac{1}{2m_2(Mx)^2} I^{n \times n}$	0	0	$-\frac{1}{2m_1(Mx)^2} I^{n \times n}$
Q_{top}	$-\frac{1}{2m_1(Mx)^2} I^{n \times n}$	0	0	$-\frac{1}{2m_2(Mx)^2} I^{n \times n}$

6.2 Truncated Octagonal-Based Pyramid Dot

We consider a truncated octagonal-based pyramid quantum dot [11] which is embedded in the center of another quadrangular materials. According to *time-independent Schrödinger equation*, the 3D model problem and boundary conditions are also (6.1) and (6.3), but with the interface conditions:

$$\begin{aligned}
 \frac{1}{m_2} \frac{\partial u}{\partial x} \Big|_{O_{\text{left}}^-} &= \frac{1}{m_1} \frac{\partial u}{\partial x} \Big|_{O_{\text{left}}^+}, & \frac{1}{m_1} \frac{\partial u}{\partial x} \Big|_{O_{\text{right}}^-} &= \frac{1}{m_2} \frac{\partial u}{\partial x} \Big|_{O_{\text{right}}^+} \\
 \frac{1}{m_2} \frac{\partial u}{\partial x} \Big|_{O_{S_1}^-} &= \frac{1}{m_1} \frac{\partial u}{\partial x} \Big|_{O_{S_1}^+}, & \frac{1}{m_1} \frac{\partial u}{\partial x} \Big|_{O_{S_2}^-} &= \frac{1}{m_2} \frac{\partial u}{\partial x} \Big|_{O_{S_2}^+} \\
 \frac{1}{m_2} \frac{\partial u}{\partial x} \Big|_{O_{S_3}^-} &= \frac{1}{m_1} \frac{\partial u}{\partial x} \Big|_{O_{S_3}^+}, & \frac{1}{m_1} \frac{\partial u}{\partial x} \Big|_{O_{S_4}^-} &= \frac{1}{m_2} \frac{\partial u}{\partial x} \Big|_{O_{S_4}^+} \\
 \frac{1}{m_2} \frac{\partial u}{\partial y} \Big|_{O_{\text{fwd}}^-} &= \frac{1}{m_1} \frac{\partial u}{\partial y} \Big|_{O_{\text{fwd}}^+}, & \frac{1}{m_1} \frac{\partial u}{\partial y} \Big|_{O_{\text{bwd}}^-} &= \frac{1}{m_2} \frac{\partial u}{\partial y} \Big|_{O_{\text{bwd}}^+}
 \end{aligned} \tag{6.8}$$

$$\frac{1}{m_2} \frac{\partial u}{\partial z} \Big|_{O_{\text{btm}}^-} = \frac{1}{m_1} \frac{\partial u}{\partial z} \Big|_{O_{\text{btm}}^+}, \quad \frac{1}{m_1} \frac{\partial u}{\partial z} \Big|_{O_{\text{top}}^-} = \frac{1}{m_1} \frac{\partial u}{\partial z} \Big|_{O_{\text{top}}^+}$$

as shown in Figure 6.2.

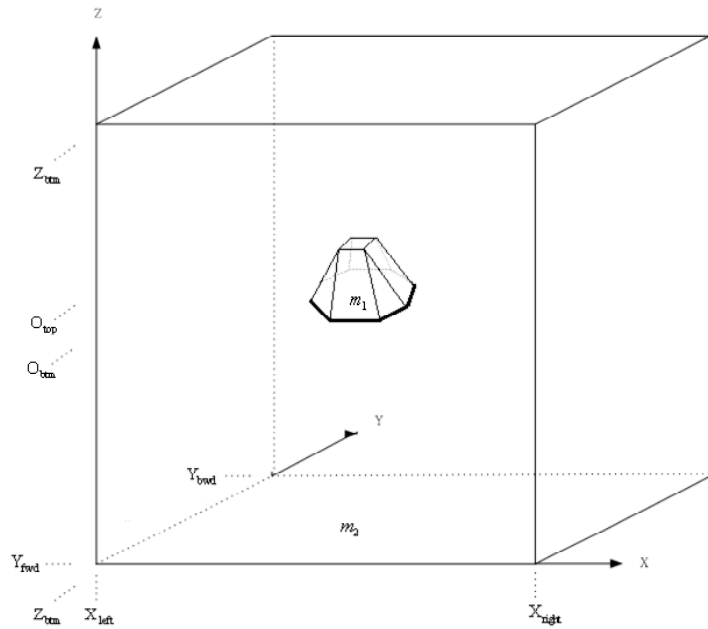


Figure 6.2 (a) Structure schema of a truncated octagonal-based pyramid dot.

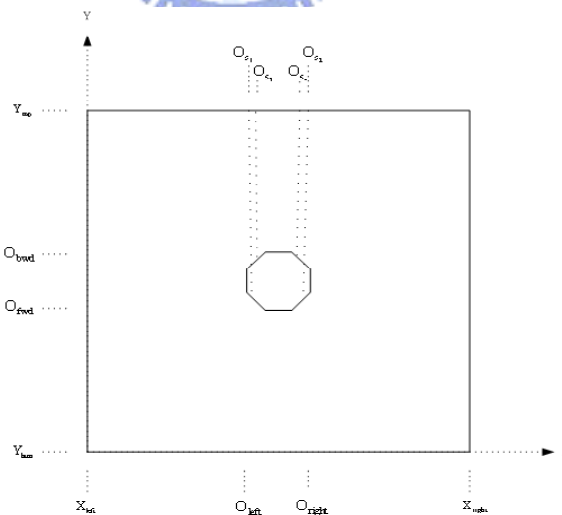


Figure 6.2 (b) Structure schema of a cross-section for X-Y plane.

6.2.1 Discretization

With the same trick, the central finite difference approximation for the model problem (6.1) is still (6.4), but the interface conditions (6.8) with quadratic interface approximation can be approximated as follows:

and

$$\alpha_i = \frac{3\tilde{z}^2}{m_1(Mx)^2}, \quad \beta_i = -\frac{\tilde{z}^2}{2m_1(Mx)^2}, \quad \gamma_i = -\frac{\tilde{z}^2}{2m_1(Mx)^2}$$

Case (iii): If the matrices $B_{i;k}$, $E_{i;k}$, $S_{i;k}$, $G_{i;k}$, $H_{i;k}$ involve the interface, the matrices $B_{i;k}$, $E_{i;k}$, $S_{i;k}$, $G_{i;k}$, $H_{i;k}$, are chosen from the three cases described in Table 6.2.

Table 6.2
Possible choices of matrices $B_{i;k}$, $E_{i;k}$, $S_{i;k}$, $G_{i;k}$, $H_{i;k}$ involving interface.

Interface type	$S_{i;k}$			
	β_i	α_i	γ_i	
O_{left}	$-\frac{\tilde{z}^2}{2m_2(Mx)^2}$	$\frac{\tilde{z}^2}{2m_1(Mx)^2} + \frac{\tilde{z}^2}{2m_2(Mx)^2} + \frac{1}{2}V$	$-\frac{\tilde{z}^2}{2m_1(Mx)^2}$	
O_{right}	$-\frac{\tilde{z}^2}{2m_1(Mx)^2}$	$\frac{\tilde{z}^2}{2m_1(Mx)^2} + \frac{\tilde{z}^2}{2m_2(Mx)^2} + \frac{1}{2}V$	$-\frac{\tilde{z}^2}{2m_2(Mx)^2}$	
O_{S_1}	$-\frac{\tilde{z}^2}{2m_2(Mx)^2}$	$\frac{\tilde{z}^2}{2m_1(Mx)^2} + \frac{\tilde{z}^2}{2m_2(Mx)^2} + \frac{1}{2}V$	$-\frac{\tilde{z}^2}{2m_1(Mx)^2}$	
O_{S_2}	$-\frac{\tilde{z}^2}{2m_1(Mx)^2}$	$\frac{\tilde{z}^2}{2m_1(Mx)^2} + \frac{\tilde{z}^2}{2m_2(Mx)^2} + \frac{1}{2}V$	$-\frac{\tilde{z}^2}{2m_2(Mx)^2}$	
O_{S_3}	$-\frac{\tilde{z}^2}{2m_2(Mx)^2}$	$\frac{\tilde{z}^2}{2m_1(Mx)^2} + \frac{\tilde{z}^2}{2m_2(Mx)^2} + \frac{1}{2}V$	$-\frac{\tilde{z}^2}{2m_1(Mx)^2}$	
O_{S_4}	$-\frac{\tilde{z}^2}{2m_1(Mx)^2}$	$\frac{\tilde{z}^2}{2m_1(Mx)^2} + \frac{\tilde{z}^2}{2m_2(Mx)^2} + \frac{1}{2}V$	$-\frac{\tilde{z}^2}{2m_2(Mx)^2}$	
O_{fwd}	0	$\frac{\tilde{z}^2}{2m_1(Mx)^2} + \frac{\tilde{z}^2}{2m_2(Mx)^2} + \frac{1}{2}V$	0	
O_{bwd}	0	$\frac{\tilde{z}^2}{2m_1(Mx)^2} + \frac{\tilde{z}^2}{2m_2(Mx)^2} + \frac{1}{2}V$	0	
O_{btm}	0	$\frac{\tilde{z}^2}{2m_1(Mx)^2} + \frac{\tilde{z}^2}{2m_2(Mx)^2} + \frac{1}{2}V$	0	
O_{top}	0	$\frac{\tilde{z}^2}{2m_1(Mx)^2} + \frac{\tilde{z}^2}{2m_2(Mx)^2} + \frac{1}{2}V$	0	

Interface type	$B_{i;k}$	$G_{i;k}$	$H_{i;k}$	$E_{i;k}$
O_{left}	0	0	0	0
O_{right}	0	0	0	0
O_{S_1}	0	0	0	0
O_{S_2}	0	0	0	0
O_{S_3}	0	0	0	0
O_{S_4}	0	0	0	0
O_{fwd}	0	$-\frac{\tilde{z}^2}{2m_2(Mx)^2} I^{n \times n}$	$-\frac{\tilde{z}^2}{2m_1(Mx)^2} I^{n \times n}$	0
O_{bwd}	0	$-\frac{\tilde{z}^2}{2m_1(Mx)^2} I^{n \times n}$	$-\frac{\tilde{z}^2}{2m_2(Mx)^2} I^{n \times n}$	0
O_{btm}	$-\frac{\tilde{z}^2}{2m_2(Mx)^2} I^{n \times n}$	0	0	$-\frac{\tilde{z}^2}{2m_1(Mx)^2} I^{n \times n}$
O_{top}	$-\frac{\tilde{z}^2}{2m_1(Mx)^2} I^{n \times n}$	0	0	$-\frac{\tilde{z}^2}{2m_2(Mx)^2} I^{n \times n}$

7 Convergency of The Smallest Eigenvalue

If we use central finite difference discretization at the non-interface, and use quadratic interface approximation at the interface, we can prove that the convergency of the smallest eigenvalue for the model equation (2.1) is $O(h^2)$.

7.1 1D Model

7.1.1 Convergency of Eigenvector

According to model equation (2.1), we know:

$$u(x) = \frac{1}{\lambda - V(x)} \frac{d^2 u(x)}{dx^2} \quad (7.1)$$

And with central finite difference method, the second differential term of approximation solution \hat{u} is thus:

$$\frac{d^2 \hat{u}(x_i)}{x^2} \approx \frac{\hat{u}^{i+1} - 2\hat{u}^i + \hat{u}^{i-1}}{(M x)^2} \quad (7.2)$$

where $\hat{u}^i = \hat{u}(x_i)$. By Taylor's expansion, the second differential term of the exact solution u is thus:

$$u^{i-1} = u^i + \frac{u_x^i}{1!}(-M x) + \frac{u_{xx}^i}{2!}(-M x)^2 + \frac{u_{xxx}^i}{3!}(-M x)^3 + C_1 O(M x^4) \quad (7.3)$$

$$u^{i+1} = u^i + \frac{u_x^i}{1!}(M x) + \frac{u_{xx}^i}{2!}(M x)^2 + \frac{u_{xxx}^i}{3!}(M x)^3 + C_2 O(M x^4) \quad (7.4)$$

(7.3)+(7.4)

$$u^{i-1} + u^{i+1} = 2u^i + u_{xx}^i(M x)^2 + C_3 O(M x^4)$$

$$u_{xx}^i = \frac{u^{i-1} - 2u^i + u^{i+1}}{(M x)^2} + C_3 O(M x^2) \quad (7.5)$$

where $u^i = u(x_i)$ and $C_3 = C_1 + C_2$. From (7.1), (7.2) and (7.5), we get the convergency of \hat{u} and u at the non-interface :

$$\|\hat{u}^i - u^i\|_1 \leq K_1 \|\hat{u}_{xx}^i - u_{xx}^i\|_1 \leq K_2 O(M x^2) \quad (7.6)$$

From quadratic interface approximation (3.2), we know:

$$\frac{1}{m_2} \left(\frac{\hat{u}^i - \hat{u}^{i-1}}{M x} + \frac{M x}{2} \hat{u}_{xx}^i \right) = \frac{1}{m_1} \left(\frac{\hat{u}^{i+1} - \hat{u}^i}{M x} + \frac{M x}{2} \hat{u}_{xx}^i \right)$$

i.e.,

$$\frac{1}{m_2} \left(\frac{\hat{u}^i - \hat{u}^{i-1}}{M x} + \frac{M x}{2} \hat{u}_{xx}^i \right) - \frac{1}{m_1} \left(\frac{\hat{u}^{i+1} - \hat{u}^i}{M x} + \frac{M x}{2} \hat{u}_{xx}^i \right) = 0 \quad (7.7)$$

by Taylor's expansion:

$$u^{i-1} = u^i + \frac{u_x^i}{1!} (-M x) + \frac{u_{xx}^i}{2!} (-M x)^2 + C_1 O(M x^3) \quad (7.8)$$

$$u^{i+1} = u^i + \frac{u_x^i}{1!} (M x) + \frac{u_{xx}^i}{2!} (M x)^2 + C_2 O(M x^3) \quad (7.9)$$

From (7.8) and (7.9)

$$\begin{aligned} & \frac{1}{m_2} u_x^i - \frac{1}{m_1} u_x^i \\ &= \frac{1}{m_2} \left(\frac{u^i - u^{i-1}}{M x} + \frac{M x}{2} u_{xx}^i \right) - \frac{1}{m_1} \left(\frac{u^{i+1} - u^i}{M x} + \frac{M x}{2} u_{xx}^i \right) + C_3 O(M x^2) \end{aligned} \quad (7.10)$$

From (7.7) and (7.10), we get the convergency of \hat{u} and u at the interface:

$$\|\hat{u}^i - u^i\|_1 \leq C_3 O(M x^2) \quad (7.11)$$

From (7.6) and (7.11), we find that every $\hat{u}(x_i)$, corresponding the every discretization point x_i , converges to $u(x_i)$ with $O(h^2)$, and therefore we know that the convergency of \hat{u} and u is $O(h^2)$.

7.1.2 Convergency of Eigenvalue

According to [10], we know the inequality equation:

$$\begin{aligned} \|u\|_1 &\leq \rho_{\bar{n}} \|u\|_2 \\ \|u\|_2 &\leq \rho_{\bar{n}} \|u\|_1 \end{aligned} \quad (7.12)$$

where $u \in C^n$. And according to [4], we know the inequality equation:

$$|\lambda_i^h - \lambda_i| \leq C \|u_i^h - u_i\|_m^2 \quad (7.13)$$

for 2mth-order problem. From (7.6), (7.11), (7.12), and (7.13), the convergency of the smallest eigenvalue is thus:

$$\begin{aligned} |\lambda_i^h - \lambda_i| &\leq C_1 \|u_i^h - u_i\|_1^2 \\ &= C_1 \| \hat{u}_i - u_i \|_1^2 \end{aligned} \quad (7.14)$$

$$\begin{aligned}
&\leq C_1(\rho \bar{n} k \hat{u}_i - u_i k_2)^2 \\
&= C_1 n k \hat{u}_i - u_i k_2^2 \\
&\leq C_1 n (\rho \bar{n} k \hat{u}_i - u_i k_1)^2 \\
&= C_1 n^2 k \hat{u}_i - u_i k_1^2 \\
&\leq C_2 \left(\frac{1}{M x^2}\right) (O(M x^2))^2 \\
&= C_2 O(h^2)
\end{aligned}$$

where $h = M x$.

Therefore, we prove the convergency of the smallest eigenvalue is $O(h^2)$.

7.2 2D Model

If we consider the model equation is two variables for 2D model as follows:

$$-\frac{\Delta u(x; y)}{2m} + V(x; y)u(x; y) = \lambda u(x; y)$$

i.e.,

$$u(x; y) = \frac{1}{\lambda - V(x; y)} \left(-\frac{\Delta u(x; y)}{2m}\right) \quad (7.15)$$

And according to central finite difference, the second differential term of approximation solution \hat{u} is thus:

$$\begin{aligned}
\frac{\partial^2 \hat{u}(x_i; y_i)}{\partial x^2} &\approx \frac{\partial^2 \hat{u}(x_i; y_i)}{\partial x^2} + \frac{\partial^2 \hat{u}(x_i; y_i)}{\partial y^2} \\
&\approx \hat{u}_{xx}^{ij} + \hat{u}_{yy}^{ij} \\
&\approx \frac{\hat{u}^{i-1j} - 2\hat{u}^{ij} + \hat{u}^{i+1j}}{(M x)^2} + \frac{\hat{u}^{ij-1} - 2\hat{u}^{ij} + \hat{u}^{ij+1}}{(M y)^2}
\end{aligned} \quad (7.16)$$

where $\hat{u}^{i,j} = \hat{u}(x_i; y_j)$. By Taylor's expansion, the second differential term of the exact solution u is thus:

$$u^{i-1j} = u^{ij} + \frac{u_x^{ij}}{1!}(-M x) + \frac{u_{xx}^{ij}}{2!}(-M x)^2 + \frac{u_{xxx}^{ij}}{3!}(-M x)^3 + C_1 O(M x^4) \quad (7.17)$$

$$u^{i+1j} = u^{ij} + \frac{u_x^{ij}}{1!}(M x) + \frac{u_{xx}^{ij}}{2!}(M x)^2 + \frac{u_{xxx}^{ij}}{3!}(M x)^3 + C_2 O(M x^4) \quad (7.18)$$

(7.17)+(7.18)

$$u_{xx}^{i,j} = \frac{u^{i-1,j} - 2u^{i,j} + u^{i+1,j}}{(Mx)^2} + C_3O(Mx^2) \quad (7.19)$$

For the same reason,

$$u_{yy}^{i,j} = \frac{u^{i,j-1} - 2u^{i,j} + u^{i,j+1}}{(My)^2} + C_4O(My^2) \quad (7.20)$$

From (7.15), (7.16), (7.19) and (7.20), we get the convergency of \hat{u} and u at the non-interface:

$$\|\hat{u}^{i,j} - u^{i,j}\|_1 \leq C_5O(Mx^2) \quad (7.21)$$

From (7.11), with the same trick, we get the convergency of \hat{u} and u at the interface:

$$\|\hat{u}^{i,j} - u^{i,j}\|_1 \leq C_6O(My^2) \quad (7.22)$$

Thus, from (7.21) and (7.22), we can get the convergency of \hat{u} and u is $O(h^2)$. From (7.14), we know that the convergency of the first eigenvalue is thus:

$$\begin{aligned} |\lambda_{i,j}^h - \lambda_{i,j}| &\leq C_1 k \hat{u}_{i,j} - u_{i,j} k_1^2 \\ &\leq C_2 O(h^2) \end{aligned} \quad (7.23)$$

Therefore, we prove the convergency of the smallest eigenvalue of the equation (7.15) is $O(h^2)$.

7.3 3D Model

If we consider the model equation is three variables for 3D model as follows:

$$\frac{-\Delta^2 u(x; y; z)}{2m} + V(x; y; z)u(x; y; z) = \lambda u(x; y; z) \quad (7.24)$$

From (7.11), (7.16), (7.19) and (7.20), with the same computation, we can get the convergency of \hat{u} and u is $O(h^2)$. From (7.14), we know the convergency of the smallest eigenvalue is thus:

$$\begin{aligned} |\lambda_{i,j;k}^h - \lambda_{i,j;k}| &\leq C_1 k \hat{u}_{i,j;k} - u_{i,j;k} k_1^2 \\ &\leq C_2 O(h^2) \end{aligned} \quad (7.25)$$

8 Numerical Results

We consider the GaAs-Al_{0.3}Ga_{0.7}As quantum well [2,6], as shown in Figure 8.1. GaAs is surrounded by Al_{0.3}Ga_{0.7}As. The effective mass $m_1 = 0.067m_0$ for GaAs, and $m_2 = 0.919m_0$ for Al_{0.3}Ga_{0.7}As, the band gap $V = 0.33\text{eV}$, the domain length is 80nm and the well length is 6nm. Numerical results are shown in Table 8.1, and Fig 8.2 and 8.3.

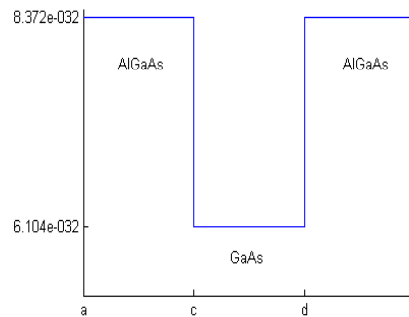


Figure 8.1 GaAs-Al_{0.3}Ga_{0.7}As quantum well for 80nm domain length and 6nm well length.

8.1 Linear Interface Approximation

Table 8.1

Numerical results of linear interface approximation.

Number of discretization points	the smallest eigenvalue
400	0.0654366759
800	0.0665192182
1600	0.0670666387
3200	0.0673417041
6400	0.0674795526
12800	0.0675485529
25600	0.0675830716

If we take the smallest eigenvalue for the number which the discretization point is 25600 as exact solution. We compute the value $\log_2 \frac{\lambda_{400n} - \lambda_{25600}}{\lambda_{800n} - \lambda_{25600}}$, where $n = 1; 2; 4; 8; 16$, and we get the convergency of $O(h)$, as shown in Table 8.2.

Table 8.2
Convergency of linear approximation.

n	$\log_2 \frac{\lambda_{400n} - \lambda_{25600}}{\lambda_{800n} - \lambda_{25600}}$
1	1:01261671
2	1:042646542
4	1:097349481
8	1:221335845
16	1:584445548



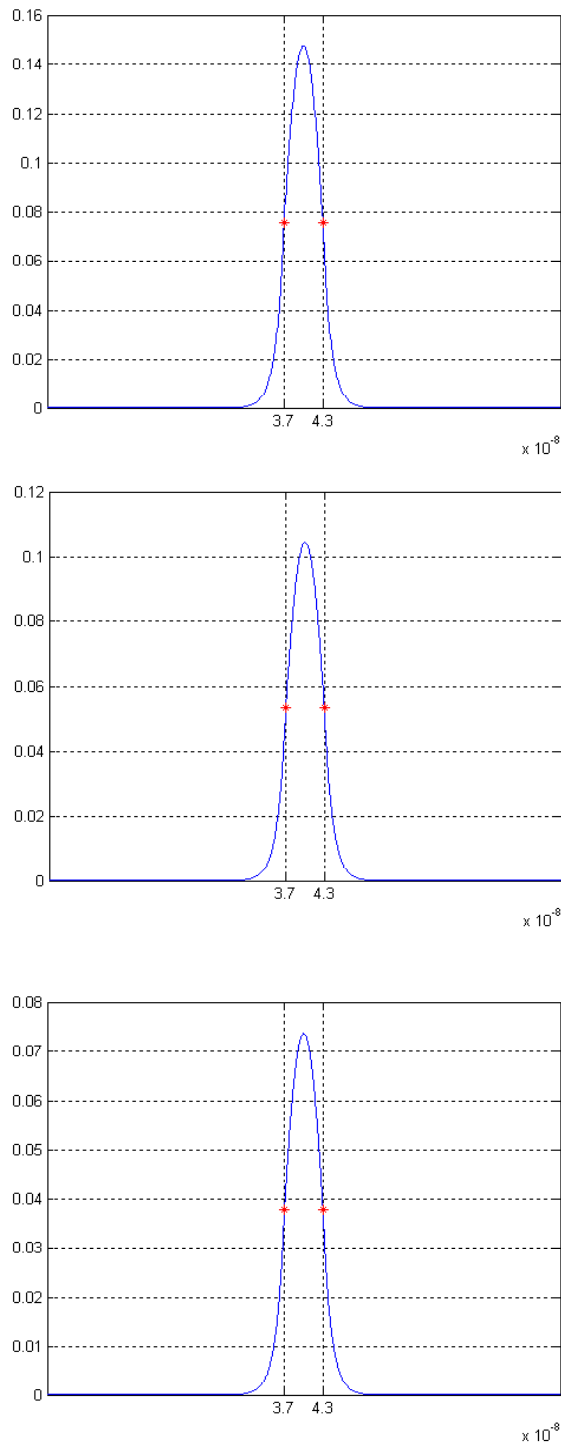


Figure 8.2 The eigenvector corresponding to $\lambda_{800}; \lambda_{1600}; \lambda_{3200}$:

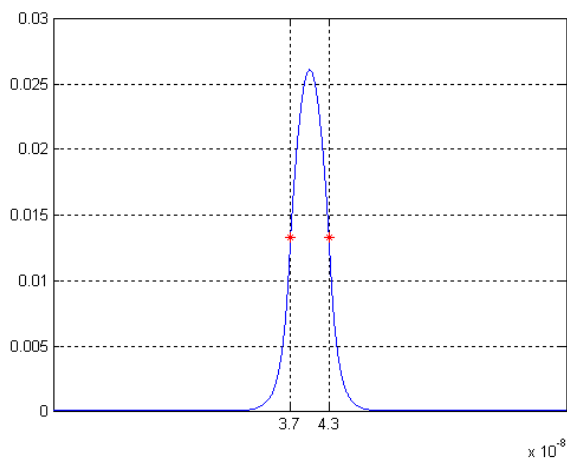
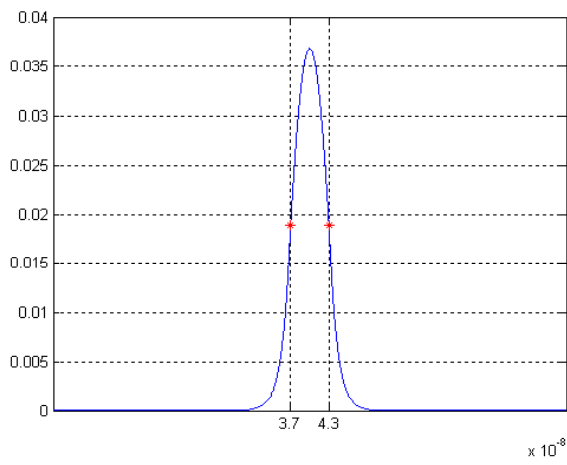
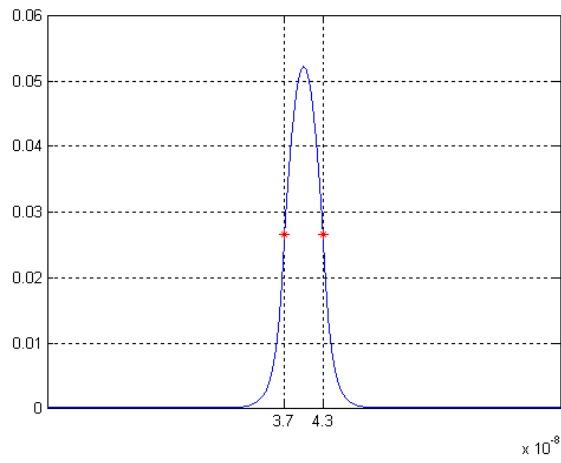


Figure 8.3 The eigenvector corresponding to $\lambda_{6400}; \lambda_{12800}; \lambda_{25600}$:

8.2 Quadratic Interface Approximation

Numerical results for this case are shown in Table 8.3, and Fig 8.4 and 8.5.

Table 8.3
Numerical results of quadratic interface approximation.

Number of discretization points	the smallest eigenvalue
400	0.0677403958
800	0.0676483810
1600	0.0676253023
3200	0.0676195279
6400	0.0676180840
12800	0.0676177231
25600	0.0676176328

Again, the smallest eigenvalue is chosen as an exact solution so that the corresponding number of the grid points is 25600. We see that the quadratic method indeed leads to quadratic convergence $O(h^2)$ as shown in Table 8.4.

Table 8.4
Convergency of quadratic approximation.

n	$\log_2 \frac{\lambda_{400n} - \lambda_{25600}}{\lambda_{800n} - \lambda_{25600}}$
1	1.997301944
2	2.003297526
4	2.016858549
8	2.070435005
16	2.320969175

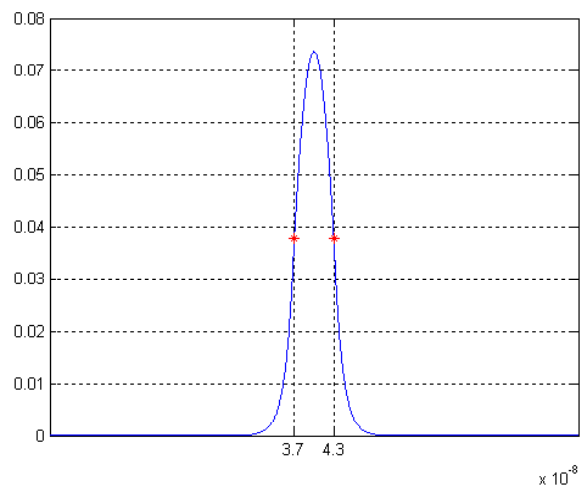
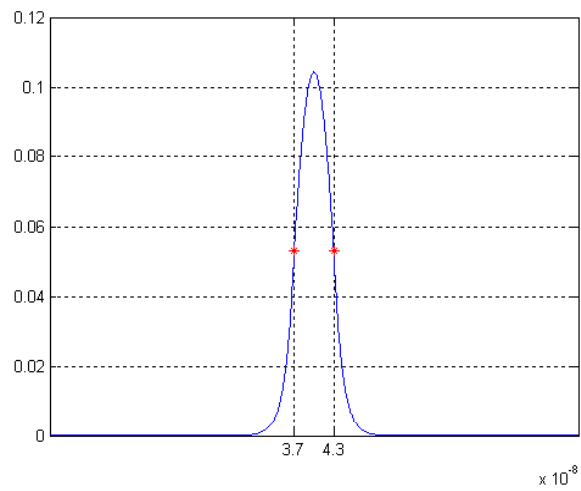
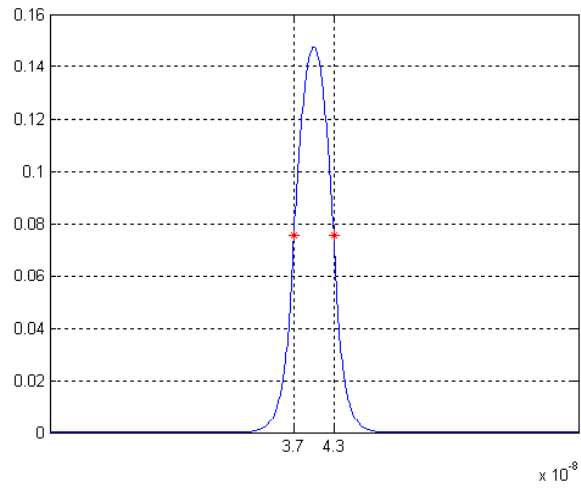


Figure 8.4 The eigenvector corresponding to $\lambda_{800}; \lambda_{1600}; \lambda_{3200}$:

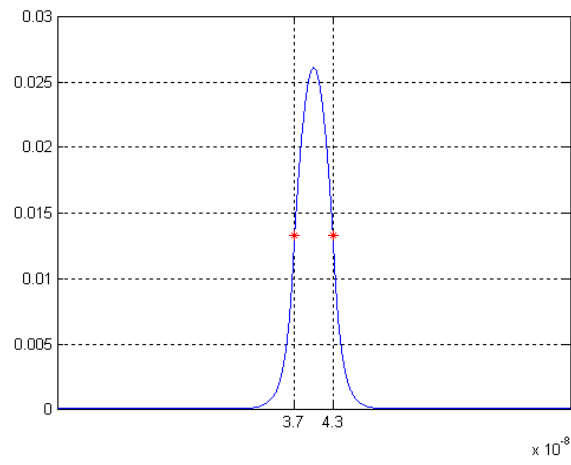
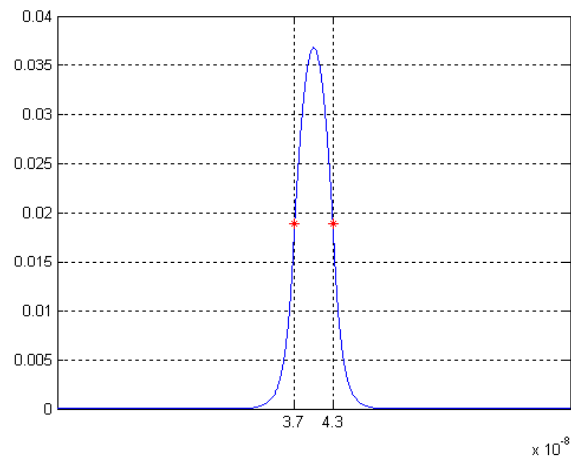
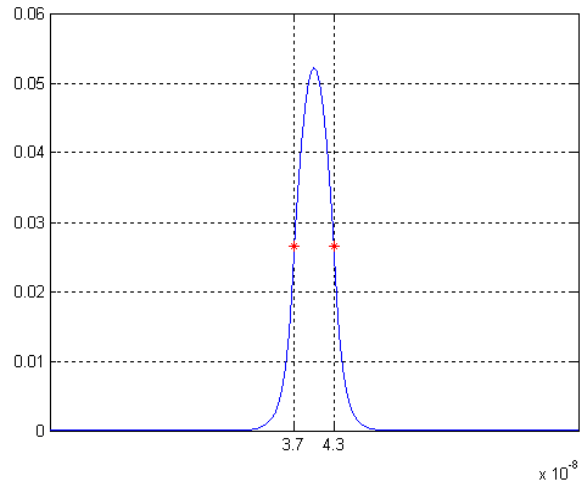


Figure 8.5 The eigenvector corresponding to $\lambda_{6400}; \lambda_{12800}; \lambda_{25600}$:

8.3 Quadratic Interface Approximation for 2D Model

From Table 8.3 and Table 8.4, we get good results with quadratic interface approximation for 1D model. Therefore, we expect that if we use quadratic interface approximation to 2D problem and we can get good results, too. For 2D problem, we still consider the GaAs-Al_{0.3}Ga_{0.7}As quantum wire, but with two forms, quadrangular wire and triangular wire.

8.3.1 Quadrangular Wire

The GaAs which is quadrangular form is embedded in the center of Al_{0.3}Ga_{0.7}As. The effective mass $m_1 = 0.067m_0$ for GaAs, and $m_2 = 0.919m_0$ for Al_{0.3}Ga_{0.7}As, the band gap $V = 0.33\text{eV}$, the domain length is 80nm and the wire length is 6nm, as shown in Figure 8.6.

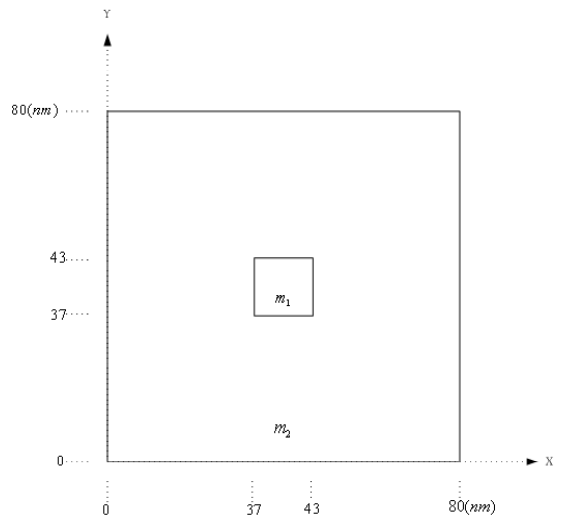


Figure 8.6 Quadrangular wire for 80nm domain length and 6nm wire length.

We compute the smallest eigenvalue of the eigenvalue system (5.6) with Linear Jacobi-Davidson method, and numerical results are shown in Table 8.5.

Table 8.5
Numerical results of quadratic interface approximation
for quadrangular wire.

Number of discretization points	the smallest eigenvalue
80	0.150776228
120	0.143535101
160	0.140267686
200	0.138426696
240	0.137249795
280	0.136433981
320	0.135835769
360	0.135378635
400	0.135018102
440	0.134726575
480	0.134486039
520	0.134284238
560	0.134112543
1000	0.133154291

Similarly, the smallest eigenvalue is chosen as an exact solution so that the corresponding number of the grid points is 1000. We see that the quadratic method indeed leads to quadratic convergence $O(h^2)$ as shown in Table 8.6.

Table 8.6
Convergency of quadratic approximation
for quadrangular wire.

n_1	n_2	α
80	120	1.305132427
120	160	1.313878089
160	200	1.342154047
200	240	1.385447265
240	280	1.441063036
280	320	1.508115132
320	360	1.586866276
360	400	1.678417846
400	440	1.784633341
440	480	1.908217490
480	520	2.052932528
520	560	2.223984138

where $\alpha = \left(\log_2 \frac{\lambda_{n_1} - \lambda_{1000}}{\lambda_{n_2} - \lambda_{1000}} \right) = \left(\log_2 \frac{n_2}{n_1} \right)$.

8.3.2 Triangular Wire

In this case, we consider that the GaAs embedded in the center of $\text{Al}_{0.3}\text{Ga}_{0.7}\text{As}$ is triangular form. The effective mass, band gap and domain length do not change, but the high length of triangular wire is 3nm, as shown in Figure 8.7.

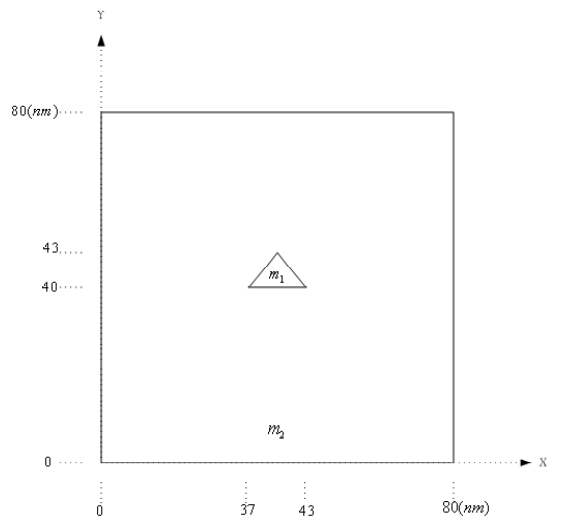


Figure 8.7 Triangular wire for 80nm domain length and 3nm triangular high length.

We still use Linear Jacobi-Davidson method to compute the smallest eigenvalue, and numerical results are shown in Table 8.7.

Table 8.7

Numerical results of quadratic interface approximation for triangular wire.

Number of discretization points	the smallest eigenvalue
80	0.229057156
120	0.228011643
160	0.226661956
200	0.225471317
240	0.224503847
280	0.223725553
320	0.223093927
360	0.222574378
400	0.222141037
440	0.221774871
480	0.221461811
520	0.221191334
560	0.220955457
1000	0.219536222

Again, the smallest eigenvalue is chosen as an exact solution so that the corresponding number of the grid points is 1000. The quadratic convergence $O(h^2)$ is

shown in Table 8.8.

Table 8.8
Convergency of quadratic approximation
for triangular wire.

n_1	n_2	α
80	120	0.286886879
120	160	0.602948987
160	200	0.819336432
200	240	0.975974275
240	280	1.105417327
280	320	1.223872831
320	360	1.340303162
360	400	1.460595640
400	440	1.589432155
440	480	1.731273778
480	520	1.891030774
520	560	2.074689085

where $\alpha = \left(\log_2 \frac{\lambda_{n_1} - \lambda_{1000}}{\lambda_{n_2} - \lambda_{1000}} \right) = \left(\log_2 \frac{n_2}{n_1} \right)$.

8.3.3 The Direction of Interface Condition

We compare the different directions of interface approximation to the triangular quantum wire. We let the direction of interface to be x-direction(x), y-direction(y) and normal-direction(n), as shown in Figure 8.8.

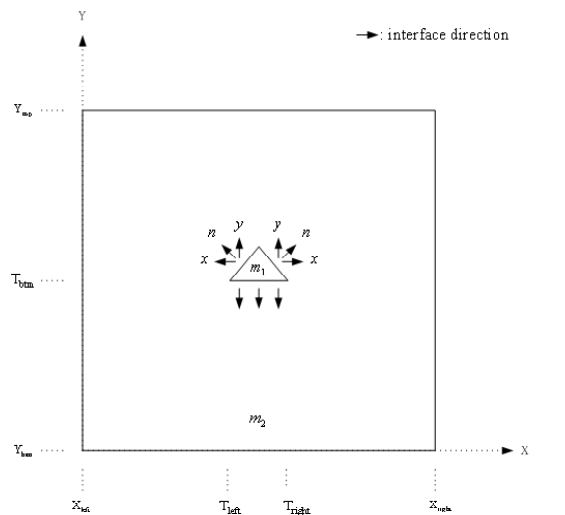


Figure 8.8 Structure schema of interface approximation for x-x, y-y, n-n directions

We compute the smallest eigenvalue with Linear Jacobi-Davidson method, and numerical results are shown in Table 8.9.

Table 8.9
Numerical results of interface approximation for x-x, y-y, n-n directions

Number of discretization points	x-direction	y-direction	n-direction
80	0.229057156	0.254449472	0.239340493
120	0.228011643	0.246422757	0.234231239
160	0.226661956	0.240833229	0.230919605
200	0.225471317	0.237146702	0.228695908
240	0.224503847	0.234582120	0.227117186
280	0.223725553	0.232706675	0.225943389
320	0.223093927	0.231279313	0.225038259
360	0.222574378	0.230158088	0.224319798
400	0.222141037	0.229254718	0.223736023
440	0.221774871	0.228511659	0.223252495
480	0.221461811	0.227889885	0.222845539
520	0.221191334	0.227362036	0.222498361
560	0.220955457	0.226908378	0.222198730
1000	0.219536222	0.224293304	0.220449095

8.4 Quadratic Interface Approximation for 3D Model

For 3D problem, we still consider the GaAs-Al_{0.3}Ga_{0.7}As quantum dot with two forms, quadrangular dot and truncated octagonal-based pyramid dot.

8.4.1 Quadrangular Dot

The GaAs embedded in the center of Al_{0.3}Ga_{0.7}As is quadrangular form, and the domain length is 80nm, the dot length is 6nm, as shown in Figure 8.9.

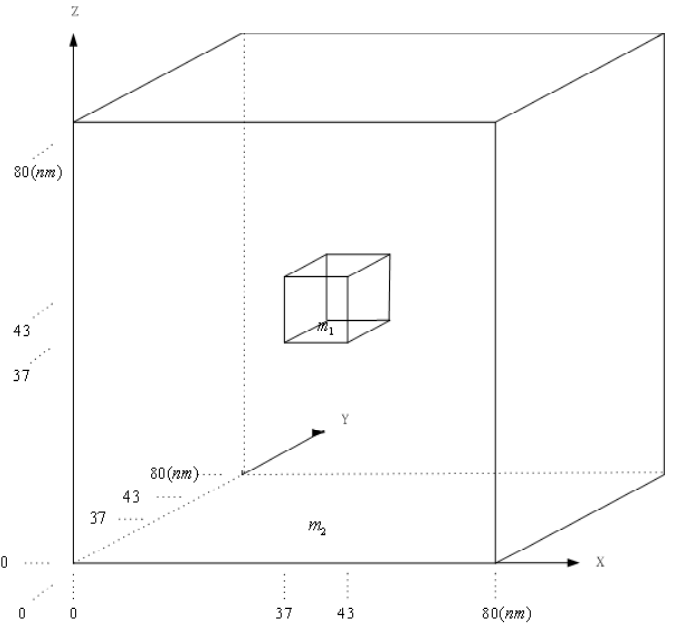


Figure 8.9 Quadrangular dot for 80nm domain length and 6nm dot length.

We still use Linear Jacobi-Davidson method to compute the smallest eigenvalue, and numerical results are shown in Table 8.10.

Table 8.10

Numerical results of quadratic interface approximation for quadrangular dot.

Number of discretization points	the smallest eigenvalue
80	0.222975522
120	0.238028478
160	0.252003562
200	0.265509664
240	0.277890995

Similarly, the smallest eigenvalue is chosen as an exact solution so that the corresponding number of the grid points is 240. The quadratic convergence $O(h^2)$ is shown in Table 8.11.

Table 8.11

Convergency of quadratic approximation for quadrangular dot.

n_1	n_2	α
80	120	0.790101724
120	160	1.500541303
160	200	3.305351448

8.4.2 Truncated Octagonal-Based Pyramid Dot

In this case, we consider that the GaAs embedded in the center of $\text{Al}_{0.3}\text{Ga}_{0.7}\text{As}$ is a truncated octagonal-based pyramid. Except the top of the dot, each cross-section of GaAs in the X-Y plane is a octagon. The domain length is still 80nm and the high length of the dot is 6nm, as shown in Figure 8.10.

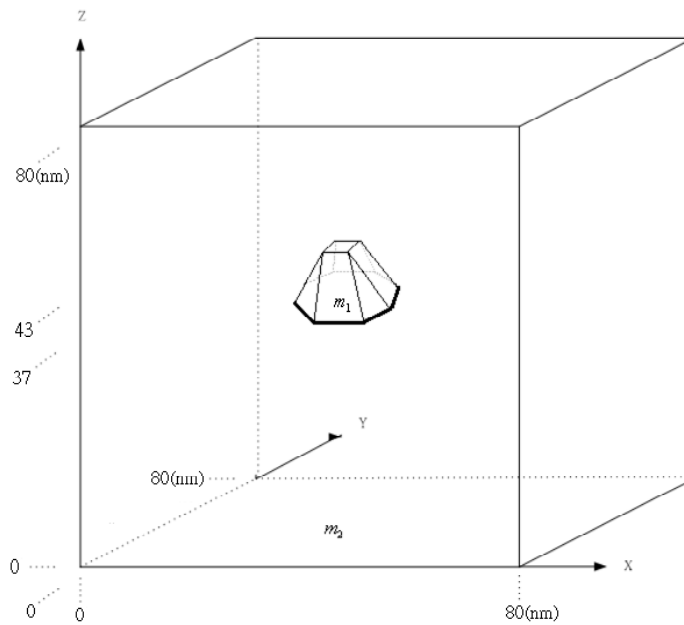


Figure 8.10 (a) Truncaetd octagonal-based pyramid dot for 80nm domain length and 6nm high length.

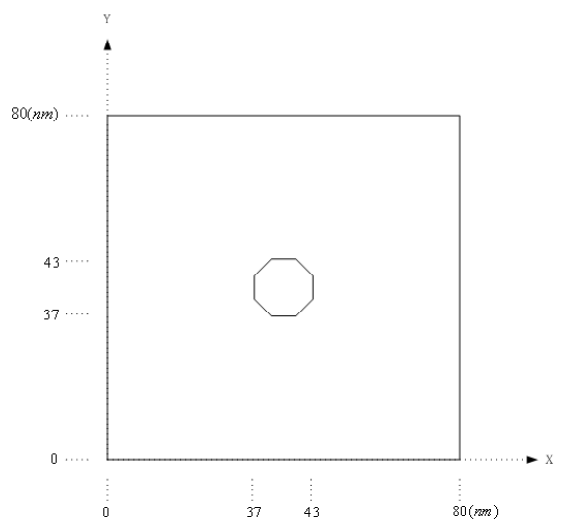


Figure 8.10 (b) Cross-section of the truncated octagonal-based pyramid dot for X-Y plane.

Again, we use Linear Jacobi-Davidson method to compute the smallest eigenvalue, and numerical results are shown in Table 8.12.

Table 8.12
 Numerical results of quadratic interface approximation
 for truncated octagonal-based pyramid dot.

Number of discretization points	the smallest eigenvalue
80	0.226957440
120	0.239821566
160	0.250414198
200	0.258812098
240	0.264974261

Again, the smallest eigenvalue is chosen as an exact solution so that the corresponding number of the grid points is 240. The quadratic convergence $O(h^2)$ is shown in Table 8.13.

Table 8.13
 Convergency of quadratic approximation
 for truncated octagonal-based pyramid dot.

n_1	n_2	α
80	120	1.018740363
120	160	1.900301524
160	200	3.853369264

Part II

Matrix Reduction

9 Introduction

In the first part, it is difficult to solve eigenvalue problems with huge matrices. However, many calculations for the huge matrix are unnecessary. Because the solution function is exponentially approaching zero beyond the confinement regions. It is shown here that the reduction factor is $(\frac{1}{4})^n$, $n = 1(1D)$, $n = 2(2D)$, $n = 3(3D)$ with the accuracy of the smallest eigenvalue up to 5 decimal point. Therefore, the method which is used to reduce the matrix and the level which we gain in reducing the matrix are very important problems. Especially the model in 2D or 3D, because the matrix is huge, it is a very important problem to reduce the calculations which are unnecessary.

10 Reduction of The Matrix

To reduce the matrix means to delete some grid points. Because the matrix is constructed by the equations of the grid points. Thus, if we want reduce the matrix, we can delete some grid points. But the position and the number of deleted points are very important. If the deleted points are in the quantum well, the accuracy of the smallest eigenvalue is affected largely. If there are too many grid points which are deleted, the error of the smallest eigenvalue would increase even though the calculator of the matrix has reduced.

10.1 Positions of Deleted Points

We find that it is much better that the positions of deleted points are far away the quantum well. Because the eigenvectors corresponding to these grid points are exponentially approaching zero. After we delete these grid points, the error of the smallest eigenvalue is still small.

However, if the positions of deleted points are in the quantum well, the error of the smallest eigenvalue is big even though we only reduce one grid point. This is because the eigenvectors corresponding to these grid points are nonzero. If we delete grid points indiscriminately, we may make big error.

10.2 Numbers of Deleted Points

How many grid points could be deleted? This seems to be very problem dependent. Because it is concerned about what accuracy you can tolerate and how big the domain is to be simulated. In our experience, the ratio of the numbers of the grid points between the inside and the outside of the well is approximately $(\frac{1}{2})^n$ for up to 5 decimal point accuracy, $n = 1; 2; 3$.

11 Numerical Results

11.1 1D Model

For 1D model, we still choose the quantum well of GaAs-Al_{0.3}Ga_{0.7}As, and the number of total grid points which we discretize is 800, and the number of grid points in the well is 60. We delete the grid points which are outside the well, and show the result in Table 11.1.

Table 11.1

The number of total grid points is 800, and the number of grid points in the well is 60.

Number of deleted points	the smallest eigenvalue
0	0.067648381
2	0.067648381
100	0.067648381
200	0.067648381
300	0.067648381
400	0.067648381
500	0.067648381
600	0.067649395
700	0.070597346

If we delete the grid points which are in the well, the result is shown in Table 11.2 as follows:

Table 11.2

The number of total grid points is 800, and the number of grid points in the well is 60.

Number of deleted points	the smallest eigenvalue
0	0.0676483810
1	0.0691423424
2	0.0706856067
3	0.0722803122
4	0.0739287095

11.2 2D Model

With the experience of 1D model, we deal with 2D problem similarly. For 2D model, we still consider the GaAs-Al_{0.3}Ga_{0.7}As quantum wire with two forms, quadrangular wire and triangular wire.

11.2.1 Quadrangular Wire

The GaAs is embedded in the center of Al_{0.3}Ga_{0.7}As, and the domain length is still 80nm, the wire length is still 6nm, as shown in Figure 11.1.

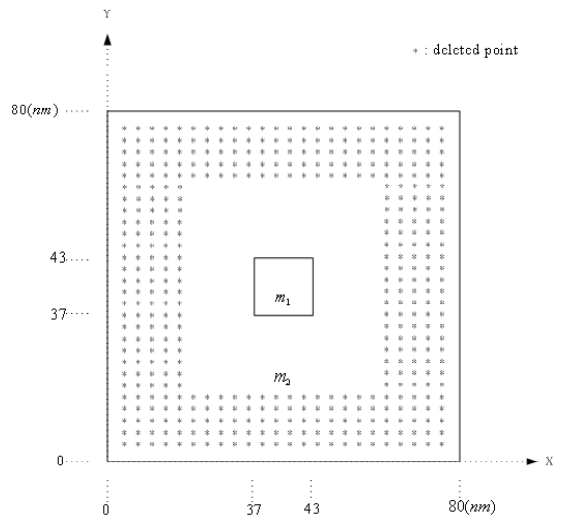


Figure 11.1 Structure schema of deleted point for the quadrangular wire.

For each side, the number of total grid points which we discretize is 800, and the number of grid points in the wire is 60. We delete the grid points which are outside the wire symmetrically, and show the result in Table 11.3.

Table 11.3

For each side, the number of total grid points is 800, and the number of grid points in the wire is 60.

Number of deleted points	the smallest eigenvalue
0	0.133454599
100	0.133454599
200	0.133454599
300	0.133454599
400	0.133454599
500	0.133454603
600	0.133459353
700	0.139817185

11.2.2 Triangular Wire

We use the same skill to triangular quantum wire which the domain length is 80nm and the high length of triangular wire is 3nm, as shown in Figure 11.2.

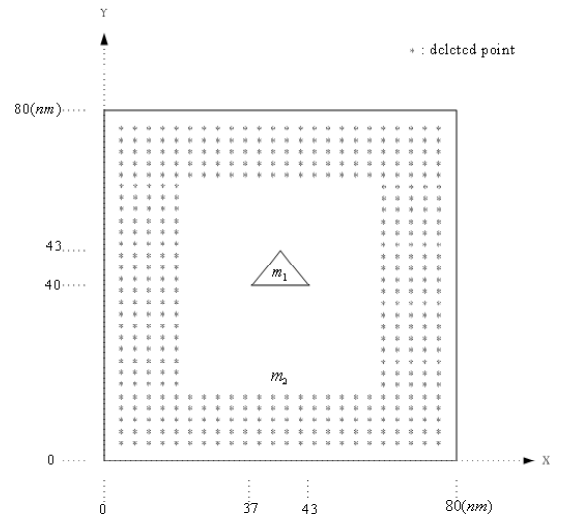


Figure 11.2 Structure schema of deleted point for the triangular wire.

Again, the number of total grid points which we discretize for each side is still 800, and the number of grid points for the high of triangular wire is 30. We show the numerical result in Table 11.4.

Table 11.4

For each side, the number of total grid points is 800, and the number of grid points for the high of triangular wire is 30.

Number of deleted points	the smallest eigenvalue
0	0.220000492
100	0.220000492
200	0.220000492
300	0.220000492
400	0.220000492
500	0.220000689
600	0.220002040
700	0.230964566

11.3 3D Model

For 3D model, we consider the GaAs-Al_{0.3}Ga_{0.7}As quantum dot with two forms, quadrangular dot and truncated octagonal-based pyramid dot.

11.3.1 Quadrangular Dot

The GaAs is embedded in the center of Al_{0.3}Ga_{0.7}As, and the domain length is 80nm; the dot length is 6nm. For each side, the number of total grid points which we discretize is 80, and the number of grid points in the dot is 6. We delete the grid points which are outside the dot symmetrically, like 2D model, and show the result in Table 11.5.

Table 11.5

For each side, the number of total grid points is 80, and the number of grid points in the dot is 6.

Number of deleted points	the smallest eigenvalue
0	0.222975522
10	0.222975522
20	0.222975522
30	0.222975523
40	0.222975524
50	0.222975662
60	0.223003735
70	0.228506895

11.3.2 Truncated Octagonal-Based Pyramid Dot

The GaAs embedded in the center of $\text{Al}_{0.3}\text{Ga}_{0.7}\text{As}$ is a truncated octagonal-based pyramid., and the domain length is 80nm; the dot length is 6nm. For each side, the number of total grid points which we discretize is still 80, and the number of grid points in the dot is 6. We still delete the grid points symmetrically, and get the result in Table 11.6.

Table 11.6

For each side, the number of total grid points is 80, and the number of grid points in the dot is 6.

Number of deleted points	the smallest eigenvalue
0	0.226957440
10	0.226957440
20	0.226957440
30	0.226957439
40	0.226957439
50	0.226957574
60	0.226984064
70	0.232934269

12 Conclusion

In the first part, we know that it is the best choice to let the discretization of the grid point at the interface to be quadratic. With this discretization, we can get the accuracy of $O(h^2)$ to the smallest eigenvalue. In the second part, to avoid the calculations which are nonnecessary, we delete some grid points, and we find that the deleted grid points which are outside the quantum well, wire, and dot are much better than those grid points which are inside the well, wire and dot.



References

- [1] R. L. Burden and J. D. Faires. *Numerical Analysis*. pp 673-683, Brooks/Cole Publishing Company, 1997.
- [2] J. H. Davies. *The Physics of Low-Dimensional Semiconductors*. pp. 80-117, Cambridge University Press, 1998.
- [3] D. R. Fokkema, G. L.G. Sleijpen, and H. A. van der Vorst. *Jacobi-Davidson style QR and QZ algorithms for the reduction of matrix pencils*. SIAM J. Sci. Comput., 20(1):94-125, 1998.
- [4] S. Gilbert and F. George J.. *An Analysis of The Finite Element Method*, Englewood Cliffs, NJ/Prentice-Hall, 1973.
- [5] L. Harris, D. J. Mowbray, M. S. Skolnick, M. Hopkinson, and G. Hill. *Emission spectra and mode structure of InAs/GaAs self-organized quantum dot lasers*. Appl. Phys. Lett., 73:969-971, 1998.
- [6] P. Harrison. *Quantum Wells, Wires and Dots*. pp. 17-70, John Wiley and Sons, Ltd., 2000.
- [7] S. Maimon, E. Finkman, G. Bahir, S. E. Schacham, J. M. Carcia, and P. M. Petroff. *Intersublevel transitions in InAs/GaAs quantum dots infrared photodetectors*. Appl. Phys. Lett., 73:2003-2005, 1998.
- [8] G. L. Sleijpen and H. A. van der Vorst. *A Jacobi-Davidson iteration method for linear eigenvalue problems*. SIAM J. Sci. Matrix Anal. Appl., 17(2):401-425, April, 1996.
- [9] J. C. Strikwerda. *Finite Difference Schemes and Partial Differential Equations*. pp. 13-23 and 53-65, Brooks/Cole Publishing Company, 1989.
- [10] J. C. Strikwerda. *Finite Difference Schemes and Partial Differential Equations*. pp. 351-363, Brooks/Cole Publishing Company, 1989.
- [11] K. Zhang, J. Falta, Th. Schmidt, Ch. Heyn, G. Materlik, and W. Hansen. *Pure Appl. Chem.*, Vol. 72, Nos. 1-2, pp. 199-207, 2000.